JSLHU
JOURNAL OF SCIENCE
OF LAC HONG UNIVERSITY

ISSN: 2525 - 2186
Tạp chí Khoa học Lạc Hồng, 2026, 27, 046-054

ẢNH HƯỞNG CỦA TỶ LỆ THAY THẾ CỐT LIỆU THÔ TÁI CHẾ ĐẾN KHẢ NĂNG CHỊU NÉN DỌC TRỤC CỦA CỘT BÊ TÔNG CỐT THÉP TRONG ĐIỀU KIỆN BẢO DƯỠNG NÓNG KHÔ

Nguyễn Khánh Hùng*, Nguyễn Trần Toàn, Hồ Ngọc Hương Trang
Trường Đại học Lạc Hồng, số 10 Huỳnh Văn Nghệ, phường Trấn Biên, TP. Đồng Nai, Việt Nam
*Tác giả liên hệ: nguyenkhanhhung@lhu.edu.vn

THÔNG TIN BÀI BÁO

Ngày nhận:	13/07/2026
Ngày hoàn thiện:	21/08/2026
Ngày chấp nhận:	26/08/2026
Ngày đăng:	30/08/2026

TỪ KHÓA

Cốt liệu thô tái chế;
Bê tông cốt liệu tái chế;
Sức chịu tải dọc trục;
Bảo dưỡng nóng khô;
Mô phỏng phần tử hữu hạn.

TÓM TẮT

Nghiên cứu này đánh giá ứng xử chịu nén dọc trục của cột bê tông cốt thép sử dụng cốt liệu thô tái chế trong điều kiện bảo dưỡng nóng khô. Cốt liệu thô tái chế được sử dụng để thay thế cốt liệu thô tự nhiên với các tỷ lệ 0%, 25% và 45%. Với mỗi tỷ lệ thay thế, ba mẫu lập phương và ba mẫu cột được bảo dưỡng ở 35 °C, độ ẩm tương đối 46% và thí nghiệm ở 28 ngày tuổi. Mẫu lập phương được dùng để xác định cường độ chịu nén của bê tông, trong khi mẫu cột được thí nghiệm nén dọc trục để xác định sức chịu tải lớn nhất. Các mô hình phần tử hữu hạn được xây dựng trong Abaqus. So với nhóm đối chứng, cường độ chịu nén của bê tông giảm 4,03% và 7,45%, trong khi sức chịu tải của cột giảm 4,64% và 6,78% tương ứng với các tỷ lệ thay thế 25% và 45%. Việc thay thế cốt liệu thô tái chế không làm thay đổi cơ bản dạng phá hoại chịu nén của cột. Các mô hình phần tử hữu hạn tái hiện được xu hướng giảm sức chịu tải nhưng dự báo cao hơn kết quả thí nghiệm, với sai lệch tuyệt đối trung bình 6,91%. Kết quả nghiên cứu cung cấp cơ sở thực nghiệm và mô phỏng số, bước đầu cho việc xem xét sử dụng cốt liệu thô tái chế trong cột bê tông cốt thép ngắn chịu nén trong điều kiện bảo dưỡng nóng khô.

EFFECT OF RECYCLED COARSE AGGREGATE REPLACEMENT RATIO ON THE AXIAL COMPRESSIVE CAPACITY OF REINFORCED CONCRETE COLUMNS UNDER HOT AND DRY CURING

Nguyen Khanh Hung*, Nguyen Tran Toan, Ho Ngoc Huong Trang
Lac Hong University, 10 Huynh Van Nghe, Tran Bien ward, Dong Nai City, Viet Nam
*Corresponding Author: nguyenkhanhhung@lhu.edu.vn

ARTICLE INFO

Received:	Jul 13th, 2026
Revised:	Aug 21st, 2026
Accepted:	Aug 26th, 2026
Published:	Aug 30th, 2026

KEYWORDS

Recycled coarse aggregate;
Recycled aggregate concrete;
Axial compression;
Hot and dry curing;
Finite element modeling.

ABSTRACT

This study evaluates the axial compressive behavior of reinforced concrete columns incorporating recycled coarse aggregate under hot and dry curing conditions. Recycled coarse aggregate was used to replace natural coarse aggregate at replacement ratios of 0%, 25%, and 45%. For each replacement ratio, three cube specimens and three column specimens were cured at 35 °C and 46% relative humidity and tested at 28 days. The cube specimens were used to determine the concrete compressive strength, while the column specimens were tested under axial compression to determine the maximum load carrying capacity. Finite element models were developed in Abaqus. Compared with the control group, concrete compressive strength decreased by 4.03% and 7.45%, while column capacity decreased by 4.64% and 6.78% for the 25% and 45% RCA replacement levels, respectively. RCA replacement did not fundamentally change the compression failure mode of the columns. The finite element models reproduced the decreasing trend in load carrying capacity but overpredicted the experimental results, with a mean absolute error of 6.91%. The results provide preliminary experimental and numerical evidence for considering recycled coarse aggregate in short reinforced concrete columns under hot and dry curing conditions.

Available online at: https://lhj.vn

1. Introduction

The rapid growth of urban construction activity has increased the demand for natural aggregates and generated large quantities of construction and demolition waste. In Hanoi, Vietnam, construction solid waste was estimated at 4,186 tons per day in 2021 and was forecast to reach 9,431 tons per day in 2025 [1]. Reusing waste concrete as recycled coarse aggregate (RCA) is a practical approach for reducing the consumption of natural aggregate, limiting construction waste disposal, and supporting circular material use in the construction sector [1], [2].

RCA is produced by crushing and processing waste concrete into aggregate suitable for new concrete. RCA particles usually contain original natural aggregate, residual old mortar, and old interfacial transition zones from the parent concrete. The attached old mortar is generally more porous and more absorptive than natural aggregate, and it may contain microcracks generated during demolition, crushing, and processing [2], [3], [4]. These characteristics can reduce aggregate density, increase water absorption, and introduce more inconsistency into the concrete matrix [3], [5]. Consequently, concrete containing RCA may show reduced compressive strength and greater variability, especially as the replacement ratio increases.

Recent Vietnamese studies provide useful evidence for evaluating RCA under local material and construction conditions. Dang et al. investigated concrete using recycled aggregate from waste concrete for rural road applications and reported that strength reduction was small when the replacement level was below 30%, whereas higher replacement ratios caused clearer strength loss [6]. Toi et al. presented a case study on recycled aggregate concrete with target strength classes from B20 to B35 and replacement ratios from 0% to 100%, showing that moderate RCA replacement could still satisfy target strength requirements when mixture proportioning and workability were properly controlled [7]. These studies support the practical feasibility of RCA concrete in Vietnam, but they also indicate that replacement ratio, aggregate quality, and mixture control remain critical.

Regional reviews have shown the need for more data on recycled aggregate concrete in structural members under conditions relevant to Southeast Asian practice [8]. Existing column studies provide useful evidence at the member level, but additional data are still needed for short reinforced concrete columns using locally sourced RCA [9], [10]. The curing environment is another important issue. Hot weather concreting can increase concrete temperature, accelerate moisture loss, reduce workability, affect setting, and influence early strength development [11]. Under a hot and dry environment, both the moisture demand of RCA and external water loss may affect the development of the cementitious matrix. In the present study, all specimens were cured under the same hot and dry condition.

This study investigates the axial compressive behavior of short reinforced concrete columns made with RCA under a controlled hot and dry curing condition. Three RCA replacement ratios were used: 0%, 25%, and 45%. For each replacement level, cube specimens were tested at 28 days to determine concrete compressive strength, and reinforced concrete column specimens were tested under monotonic axial compression to determine the maximum axial load, $P_{\max}$. All specimens were cured at 35 °C and 46% relative humidity. Abaqus finite element models were developed to compare numerical predictions with the experimental capacity trend and observed damage patterns.

The objectives of the study are to evaluate the influence of RCA replacement ratio on 28 day concrete compressive strength, quantify the corresponding change in column axial capacity, examine the relationship between material strength reduction and member capacity reduction, and assess whether the finite element model can reproduce the observed trend. The study provides experimental and numerical evidence for RCA reinforced concrete columns under a hot and dry curing condition.

2. Materials and Methods

2.1 Experimental program

The main experimental variable was the replacement ratio of natural coarse aggregate by RCA. Three replacement ratios were considered: 0%, 25%, and 45%. The 0% group was used as the control group, while the 25% and 45% groups were used to evaluate the effect of partial RCA replacement. All column specimens had the same geometry, reinforcement arrangement, target concrete grade, fabrication procedure, curing condition, and loading method.

Two specimen types were prepared. The first type consisted of 150 × 150 × 150 mm concrete cubes used to determine the compressive strength at 28 days. The second type consisted of short reinforced concrete columns tested under monotonic axial compression to determine the maximum axial load, $P_{\max}$. Each RCA replacement level included three cube specimens and three column specimens, giving a total of 9 cube specimens and 9 reinforced concrete column specimens, as shown in Table 1.

***Table 1**. Experimental matrix and specimen notation*

Group	RCA replacement ratio (%)	Cube specimens	Column specimens
MV00, CV00	0	3	3
MV25, CV25	25	3	3
MV45, CV45	45	3	3

In the specimen notation, MV refers to cube specimens used for concrete compressive strength tests, while CV refers to reinforced concrete column specimens used for axial compression tests. The numbers 00, 25, and 45 indicate the percentage of natural coarse aggregate replaced by RCA.

Nghi Son PC Type I cement was used as the binder. Tap water supplied by the local municipal system was used for concrete mixing and for washing the recycled aggregate. Natural coarse aggregate was crushed stone obtained from

Tan Cang, Dong Nai Province. Natural river sand from Dong Tan, Dong Nai Province was used as fine aggregate. The main properties of the constituent materials are summarized in Table 2.

***Table 2**. Main properties of constituent materials*

Material	Property	Value
Cement	Compressive strength at 3 days	≥ 21 MPa
	Compressive strength at 28 days	≥ 40 MPa
	Initial setting time	195 min
	Final setting time	200 min
Natural coarse aggregate	Crushing value in cylinder	12.70%
	Mud, dust, and clay content	0.53%
	Abrasion value	37.40%
Sand	Mud, dust, and clay content	1.25%
	Chloride ion content	0.01%

The RCA was obtained from old concrete specimens available at the Laboratory of the Faculty of Civil Engineering, Lac Hong University. The old concrete was crushed using a compression testing machine and further broken manually with a hammer. The crushed material was sieved to obtain particles with sizes compatible with the natural coarse aggregate used in the mixtures. The RCA was washed to remove surface dust and loose particles and then dried. The RCA collection and processing procedure is shown in Figure 1.

***Figure 1**. Collection and processing procedure of RCA*

The concrete mixtures were designed for strength grade B20. The base mix proportion was selected according to the technical guidance for selecting concrete mix proportions issued by the Ministry of Construction [12]. The nominal water to cement ratio was approximately 0.55. For the RCA mixtures, part of the natural coarse aggregate was replaced by RCA by mass, while the cement, water, and sand contents were kept unchanged. The replacement ratios of 0%, 25%, and 45% were selected to represent the control, a moderate RCA replacement level, and a relatively high partial replacement level, respectively, allowing the effect of increasing RCA content to be evaluated within the experimental range. The concrete mix proportions are summarized in Table 3.

***Table 3**. Concrete mix proportions*

RCA replacement ratio (%)	Cement (kg/m^3)	Water (kg/m^3)	Sand (kg/m^3)	Natural coarse aggregate (kg/m^3)
0	355	195	645	1168
25	355	195	645	876
45	355	195	645	642.4

2.2 Specimen preparation, curing, and testing

The column specimens had a square cross section of 150 × 150 mm and a height of 300 mm. Each column was reinforced with four 12 mm diameter longitudinal bars and 6 mm diameter closed ties spaced at 45 mm along the column height. The concrete cover was 20 mm. The yield strengths of the longitudinal bars and transverse ties were 495 MPa and 270 MPa, respectively. The column geometry and reinforcement details are shown in Figure 2.

***Figure 2.** Geometry and reinforcement details of the reinforced concrete column specimen*

The constituent materials were prepared before mixing. Natural aggregates and RCA were stored separately to avoid unintended mixing among replacement groups. Concrete was mixed according to the designed proportions, placed into cube and column molds in layers, and compacted using a vibrator. After casting, the specimen surfaces were leveled, and each specimen was labeled according to its group. The reinforcement cages were positioned carefully in the column molds to maintain the required cover and consistency among the specimens. Immediately after casting, all specimens were transferred to an environmental room maintained at 35 °C and 46% relative humidity. The specimens were kept in the molds for approximately 24 hours, then demolded and returned to the same environmental condition until testing at 28 days.

Cube specimens were tested at 28 days to determine the concrete compressive strength according to TCVN 3118:2022 [13]. Before testing, the bearing surfaces were checked and cleaned to ensure stable contact with the compression platens. Column specimens were tested at 28 days under monotonic axial compression using a Phoenix automatic compression testing machine. Each column was placed concentrically between the compression platens to reduce eccentricity. A preliminary load of approximately 0.5 kN was applied to check contact stability, signal recording, and equipment response. The specimen was then loaded continuously at approximately 1.0 kN/s until the maximum load was reached and the specimen showed clear loss of load carrying capacity.

The column test setup included the compression machine, a data logger, and a computer used to acquire and store load and concrete strain signals. For each column specimen, one surface mounted strain gauge was attached at the center of one side face of the column. The axial compression test setup and instrumentation are shown in Figure 3.

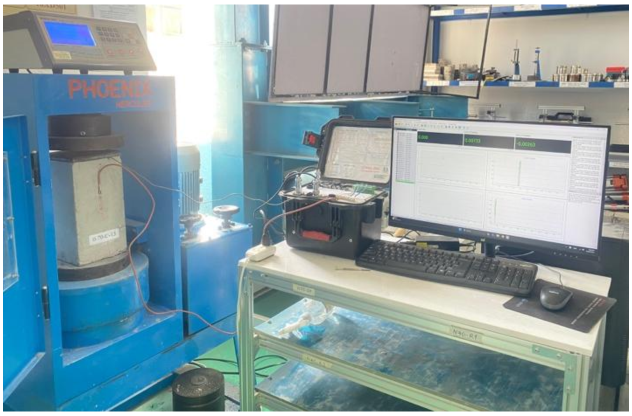

***Figure 3**. Axial compression test setup and instrumentation*

2.3 Data processing

The experimental data were processed separately for each RCA replacement group. For cube specimens, the measured compressive strength values were used to calculate the mean compressive strength at 28 days. For column specimens, the maximum recorded axial load of each specimen was used to calculate the mean column capacity of each group, $P_{\max}$. The coefficient of variation was calculated according to TCVN 10303:2025 as [14]

$$V = \frac{S}{\overline{X}} \times 100\% \tag{1}$$

where V is the coefficient of variation, S is the estimated standard deviation, and $\overline{X}$ is the mean value of the group. The coefficient of variation was used as the main scatter indicator in the Results and Discussion section.

The relative change from the control group was calculated as

$$\Delta X = \frac{X_j - X_0}{X_0} \times 100\% \tag{2}$$

where X_j is the mean value of a given RCA replacement group and X_0 is the mean value of the corresponding control group. A negative value of ΔX indicates a reduction relative to the control group. For the cube tests, X represents concrete compressive strength. For the column tests, X represents $P_{\max}$.

2.4 Finite element modeling

Finite element models were developed in Abaqus to support the interpretation of the experimental column tests. Three models were prepared, corresponding to the CV00, CV25, and CV45 column groups. The geometry and reinforcement arrangement followed the tested column specimens. The concrete was modeled using solid elements with eight nodes and reduced integration, C3D8R. The longitudinal reinforcement and transverse ties were modeled using three dimensional truss elements, T3D2. The reinforcement was embedded in the concrete using the Embedded Region constraint. The Embedded Region assumption represents perfect bond between concrete and steel and does not account for local bond slip [15].

The nonlinear behavior of concrete was represented using the Concrete Damaged Plasticity model (CDP). CDP is a continuum damage plasticity formulation used to describe inelastic concrete behavior and stiffness degradation under tensile and compressive loading [16], [17], [18]. The compressive strength inputs for the CV00, CV25, and CV45 models were 25.78 MPa, 24.74 MPa, and 23.86 MPa, respectively. These values were obtained from the mean 28-day cube compressive strengths of the corresponding MV00, MV25, and MV45 experimental groups, with three specimens tested for each group. The compressive and tensile stress strain relationships and damage variables were defined based on Eurocode 2 and the procedure proposed by Alfarah et al. [19], [20]. The CDP parameters were as follows: dilation angle of 30°, eccentricity of 0.1, $f_{b0} / f_{c0} = 1.16$, $K_c = 0.667$, and viscosity parameter $\mu = 0.001$.

The steel reinforcement was modeled as an elastic perfectly plastic material. The elastic modulus of steel was taken as 2×10^5 MPa. The yield strengths of the longitudinal bars and transverse ties were 495 MPa and 270 MPa, respectively. The concrete stress strain relationships used in the finite element models are shown in Figure 4.

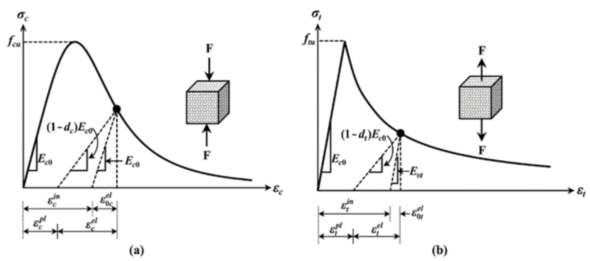

***Figure 4**. Concrete stress–strain relationships used in FEM [16]: (a) compressive behavior; (b) tensile behavior..*

Rigid plates were modeled at the top and bottom ends of the column to simulate the load transfer system. Each plate was connected to a reference point. The bottom plate was fully restrained. The top plate was restrained against horizontal displacement and rotation, while an axial displacement was imposed in the vertical direction to generate compression. The axial reaction force, RF3, at the reference point of the top plate was used to calculate the numerical compressive load. The finite element model and boundary conditions are shown in Figure 5.

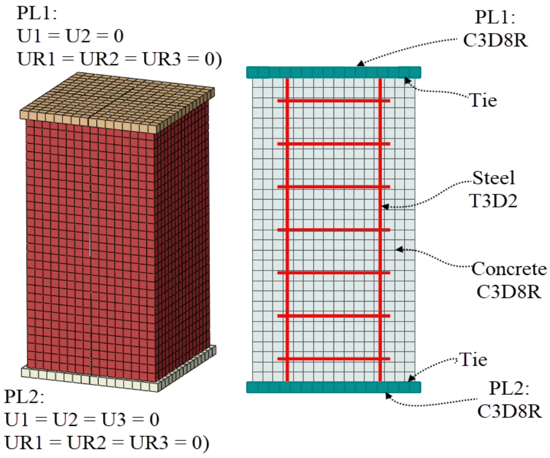

Figure 5*. Finite element model and boundary conditions*

The maximum axial capacity from the finite element model was determined as

$$P_{\max,FEM} = \max |RF3| \tag{3}$$

where $P_{\max,FEM}$ is the maximum compressive load obtained from the numerical model.

The agreement between the numerical and experimental results was evaluated using the ratio

$$R_P = \frac{P_{\max,FEM}}{P_{\max,EXP}} \tag{4}$$

and the relative error

$$\Delta_P = \frac{P_{\max,FEM} - P_{\max,EXP}}{P_{\max,EXP}} \times 100\% \tag{5}$$

where $P_{\max,EXP}$ is the mean experimental maximum axial load of the corresponding column group. The mean absolute relative error of the three models was calculated as

$$\overline{|\Delta_P|} = \frac{1}{3}\sum_{i=1}^{3} |\Delta_{P,i}| \tag{6}$$

The finite element analysis was used to evaluate whether the experimentally observed reduction in axial capacity with increasing RCA replacement could be reproduced and to compare the simulated compression damage distribution with the observed failure patterns.

3. Results and Discussion

This section presents the experimental and numerical results. The main results include the 28 day cube compressive strength, the axial compressive capacity of the reinforced concrete columns, the observed failure modes, and the comparison between the experimental and finite element results.

3.1 Concrete compressive strength and column axial capacity

Table 4 summarizes the cube compressive strength and the column axial capacity. The coefficient of variation is used as the main scatter indicator. The percentage change relative to the control group is used to evaluate the effect of RCA replacement.

Table 4*. Experimental results of cube strength and column axial capacity*

RCA replacement ratio (%)	Mean cube strength (MPa)	V_f (%)	Strength change (%)
0	25.78	1.02	0
25	24.74	0.21	-4.03
45	23.86	3.38	-7.45
RCA replacement ratio (%)	Mean $P_{\max}$ (kN)	V_P (%)	$P_{\max}$ change (%)
0	540.98	2.77	0
25	515.9	4.49	-4.64
45	504.31	3.31	-6.78

The mean cube compressive strength of the control concrete was 25.78 MPa. At 25% RCA replacement, the mean strength decreased to 24.74 MPa, corresponding to a reduction of 4.03%. At 45% RCA replacement, the mean strength decreased to 23.86 MPa, corresponding to a reduction of 7.45%. The coefficients of variation were 1.02%, 0.21%, and 3.38% for the 0%, 25%, and 45% replacement groups, respectively. These values indicate low scatter within the cube test groups.

The reduction in concrete strength can be explained by the characteristics of RCA. RCA particles generally contain residual old mortar and old interfacial transition zones from the parent concrete. The attached mortar is usually more porous and more absorptive than natural aggregate. It may also contain microcracks caused by crushing and processing. These features can create weaker zones around aggregate particles [2], [3], [4], [5]. As the RCA replacement ratio increased, these effects became more influential. This explains the gradual decrease in 28 day compressive strength observed in this study. The strength trend is consistent with previous studies on RCA concrete [6], [7]. Therefore, the reductions of 4.03% at 25% replacement and 7.45% at 45% replacement can be regarded as moderate within the tested range.

The mean axial capacity of the control column group was 540.98 kN. At 25% RCA replacement, the mean $P_{\max}$ decreased to 515.90 kN, corresponding to a reduction of 4.64%. At 45% RCA replacement, the mean $P_{\max}$ decreased to 504.31kN, corresponding to a reduction of 6.78%. The coefficients of variation of $P_{\max}$ were 2.77%, 4.49%, and 3.31% for the 0%, 25%, and 45% replacement groups, respectively. The scatter in column capacity was slightly higher than the scatter in cube strength. This is reasonable because column response can be affected by reinforcement positioning, end surface condition, loading alignment, and local cracking. The reduction in column capacity followed the same general trend as the reduction in cube compressive strength. At 25% RCA replacement, the cube strength retained 95.97% of the control value, while the column retained 95.36% of the control axial capacity. At 45% RCA replacement, the cube strength retained 92.55% of the control value, while the column retained 93.22% of the control axial capacity. This close agreement indicates that, within the tested configuration, the decrease in $P_{\max}$ was strongly related to the decrease in concrete compressive strength.

3.2 Failure modes

The column tests also included load and concrete strain acquisition using a surface mounted strain gauge and a data logging system. The representative load strain response is shown in Figure 6. The curve confirms that the acquisition system captured the strain response during axial loading.

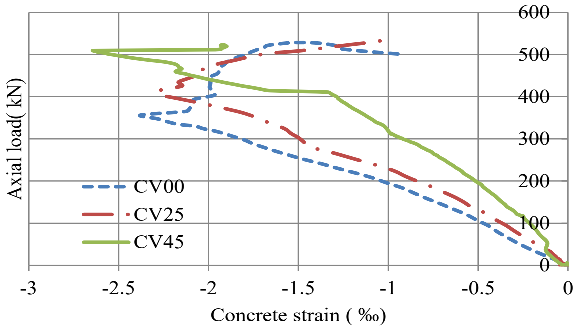

***Figure 6**. Representative load versus concrete strain response*

Representative failure modes of the column specimens are shown in Figure 7. All column groups exhibited compression dominated failure. The main observed features were vertical or slightly inclined cracks, concrete cover spalling, and local crushing near the column edges or loading end regions.

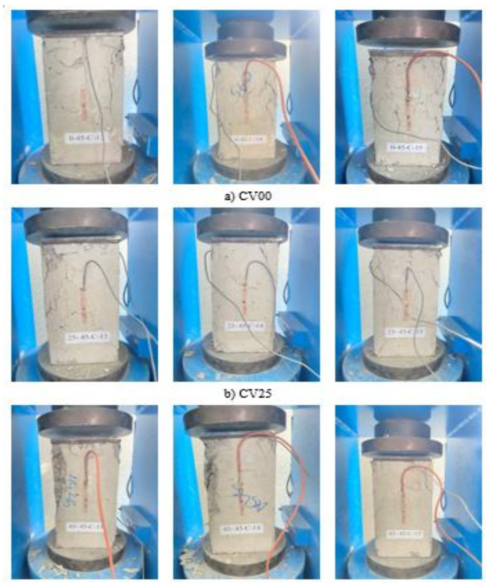

***Figure 7**. Failure modes of representative column specimens after axial compression*

The control group showed vertical cracking along the column body, followed by local cover spalling and crushing near the end regions. The 25% RCA replacement group showed a similar failure pattern. No fundamental change in the global failure mode was observed compared with the control group. The 45% RCA replacement group also failed in axial compression, but some specimens showed more visible cracking and cover spalling.

Overall, increasing the RCA replacement ratio from 0% to 45% did not change the basic failure mechanism of the reinforced concrete columns. The main difference was the severity and visibility of local damage, especially in the 45% replacement group. This observation agrees with the capacity results. RCA replacement reduced $P_{\max}$, but it did not cause a different form of global failure.

3.3 Experimental and FEM comparison

Table 5 compares the experimental axial capacity with the finite element prediction for each column group. The experimental value, $P_{\max,\text{EXP}}$, is the mean maximum axial load obtained from the column tests. The numerical value, $P_{\max,\text{FEM}}$, is the maximum axial load calculated from the reaction force at the reference point of the top rigid plate.

***Table 5**. Comparison between experimental and FEM axial capacity*

Group	$P_{\max,\text{EXP}}$ (kN)	$P_{\max,\text{FEM}}$ (kN)	R_P	Error (%)
CV00	540.98	568.58	1.051	5.1
CV25	515.9	555.53	1.077	7.68
CV45	504.31	544.45	1.08	7.96
Mean			1.069	6.91

The FEM model predicted axial capacities of 568.58 kN, 555.53 kN, and 544.45 kN for CV00, CV25, and CV45, respectively. The corresponding experimental values were 540.98 kN, 515.90 kN, and 504.31 kN. The FEM to experiment ratio ranged from 1.051 to 1.080, and the mean absolute relative error was 6.91%. Thus, the numerical model overpredicted the experimental capacity for all three groups. This comparison is shown in Figure 8.

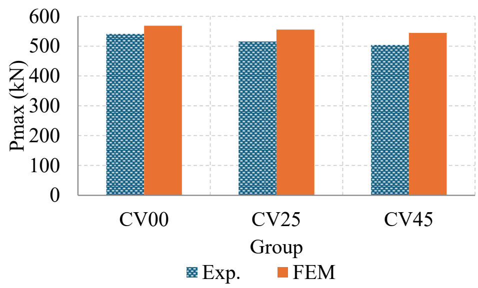

***Figure 8**. Experimental and FEM axial capacity comparison*

Although the FEM model overpredicted the absolute capacity, it captured the decreasing trend caused by increasing RCA replacement. Relative to the control model, the numerical capacity decreased by 2.30% for CV25 and 4.24% for CV45. The corresponding experimental reductions were 4.64% and 6.78%. Therefore, the model captured the direction of the experimental trend, but underestimated the magnitude of the capacity reduction caused by RCA replacement.

The overprediction can be explained by several modeling idealizations. First, concrete was modeled as a homogeneous continuum material. In reality, RCA concrete contains natural aggregate, recycled aggregate, residual mortar, old interfacial transition zones, new interfacial transition zones, pores, and local defects. These local heterogeneities can reduce the real load carrying capacity, but they are not explicitly represented in the finite element model. Second, the Embedded Region constraint assumes perfect bond between steel reinforcement and concrete [15]. In real specimens, local slip, microcracking around reinforcement, and imperfect bond may occur after damage develops. Third, the Concrete Damaged Plasticity model represents cracking and crushing through a continuum damage plasticity formulation [16], [17], [18]. This formulation is suitable for representing global nonlinear response and damage localization, but it does not reproduce every discrete crack or local spalling feature observed in the tests. In addition, the concrete stress strain relationships and damage variables were defined from established procedures rather than calibrated from complete stress strain tests of each concrete mixture [19], [20].

The simulated compression damage distribution is compared with the observed failure modes in Figure 9. The numerical DAMAGEC field was concentrated near the column edges, corners, and loading end regions. These zones corresponded reasonably with the observed cracking, cover spalling, and local crushing in the tested columns.

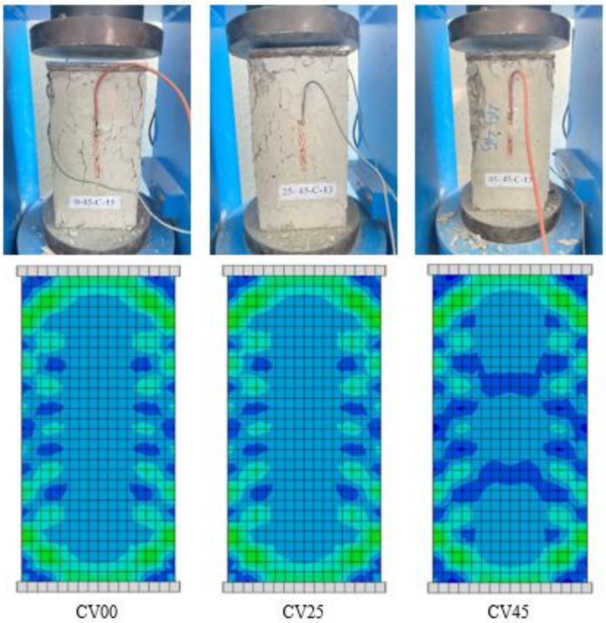

***Figure 9**. Experimental failure modes and FEM DAMAGEC distribution*

For CV00 and CV25, the simulated damage was mainly localized near the side edges and end regions. This was consistent with the observed compression dominated failure. For CV45, the model showed a wider and more continuous damage distribution in some regions. This was consistent with the more visible cracking and spalling observed in several 45% RCA specimens. However, the agreement should be interpreted at the level of general damage location and capacity trend, not as crack by crack reproduction.

4. Conclusions

This study investigated the axial compressive behavior of short reinforced concrete columns containing recycled coarse aggregate under a controlled hot and dry curing condition. RCA replacement ratios of 0%, 25%, and 45% were considered. Cube tests were used to determine concrete compressive strength, column tests were used to determine the maximum axial load, $P_{\max}$, and finite element models were developed in Abaqus using the Concrete Damaged Plasticity model. The main conclusions are as follows.

(i) RCA replacement caused a moderate reduction in concrete compressive strength. The mean cube strength decreased from 25.78 MPa for the control concrete to 24.74 MPa and 23.86 MPa for the 25% and 45% RCA mixtures, corresponding to reductions of 4.03% and 7.45%, respectively.

(ii) The axial compressive capacity of the columns decreased with increasing RCA replacement ratio. The mean $P_{\max}$ decreased from 540.98 kN for CV00 to 515.90 kN for CV25 and 504.31 kN for CV45, corresponding to reductions of 4.64% and 6.78%, respectively. The reduction in column capacity followed the same general trend as the reduction in cube compressive strength.

(iii) RCA replacement did not change the main failure mode of the short reinforced concrete columns. All column groups showed compression dominated failure, with vertical or slightly inclined cracks, concrete cover spalling, and local crushing near the column edges or loading end regions.

(iv) The finite element models captured the decreasing trend in axial capacity and showed reasonable agreement with the observed damage zones. However, the models overpredicted the experimental capacities, with FEM to experiment ratios from 1.051 to 1.080 and a mean absolute relative error of 6.91%.

Overall, the results provide preliminary experimental and numerical evidence that partial RCA replacement can be considered for short reinforced concrete compression members under the adopted hot and dry curing condition. Within the tested range, the 25% RCA replacement level caused small reductions in both concrete strength and column capacity, while the 45% replacement level still retained more than 92% of the control cube strength and more than 93% of the control column capacity.

Since no standard curing control group was included, the independent effect of hot and dry curing could not be isolated. Future studies should include more RCA sources, larger specimen numbers, standard curing control specimens, different column geometries, different reinforcement ratios, and more complete strain and displacement measurements.

3. Acknowledgements

The authors sincerely acknowledge Lac Hong University for supporting this study under grant number LHU-RF-TE-26-05-04.

4. References

[1] Hạnh V. K. and Huyền N. T., "Nghiên cứu quản lý chất thải rắn xây dựng tại hà nội theo định hướng kinh tế tuần hoàn," *Tạp Chí Môi Trường*, no. 1, pp. 3–7, 2022.

[2] R. V. Silva, J. de Brito, and R. K. Dhir, "Properties and composition of recycled aggregates from construction and demolition waste suitable for concrete production," *Constr. Build. Mater.*, vol. 65, pp. 201–217, 2014
DOI: 10.1016/j.conbuildmat.2014.04.117

[3] K. P. Verian, W. Ashraf, and Y. Cao, "Properties of recycled concrete aggregate and their influence in new concrete production," *Resour. Conserv. Recycl.*, vol. 133, pp. 30–49, 2018
DOI: 10.1016/j.resconrec.2018.02.005.

[4] S. A. Memon, Z. Bekzhanova, and A. Murzakarimova, "A review of improvement of interfacial transition zone and adherent mortar in recycled concrete aggregate," *Buildings*, vol. 12, no. 10, p. 1600, 2022
DOI: 10.3390/buildings12101600

[5] M. Etxeberria, E. Vázquez, A. Marí, and M. Barra, "Influence of amount of recycled coarse aggregates and production process on properties of recycled aggregate concrete," *Cem. Concr. Res.*, vol. 37, no. 5, pp. 735–742, 2007
DOI: 10.1016/j.cemconres.2007.02.002.

[6] H. Q. Dang, P. D. Hoang, T. A. Bui, T. H. T. Ngo, and A. T. Chu, "Research on the possibility of applying concrete using recycled aggregates from waste concrete to build rural roads," *J. Min. Earth Sci. Vol*, vol. 61, no. 6, pp. 66–73, 2020
DOI: 10.46326/JMES.HTCS2020.09.

[7] Tới P. T., Công V. C., and Tuyến T. N., "Nghiên cứu điển hình về bê tông cốt liệu tái chế từ phế thải xây dựng tại hà nội," *Tạp Chí Vật Liệu Và Xây dựng-Bộ Xây Dựng*, vol. 15, no. 5, pp. 108-Trang 115, 2025, doi: 10.54772/jomc.05.2025.1148

[8] R. P. Neupane, T. Imjai, N. Makul, R. Garcia, B. Kim, and S. Chaudhary, "Use of recycled aggregate concrete in structural members: a review focused on southeast Asia," *J. Asian Archit. Build. Eng.*, vol. 24, no. 3, pp. 1197–1220, 2025
DOI: 10.1080/13467581.2023.2270029.

[9] F. A. Ali, Q. A. Hasan, and D. H. Mohammed, "Behavior of Recycled Aggregate Concrete Slender Column under Concentric Axial Loading," *E3S Web Conf.*, vol. 427, p. 02016, 2023
DOI: 10.1051/e3sconf/202342702016.

[10] T.T. Pham, K.H. Nguyen, and T.T. Nguyen, "Compressive strength of confined reinforced recycled coarse aggregate concrete columns," *GEOMATE J.*, vol. 29, no. 136, pp. 69–77, 2025
DOI: 10.21660/2025.136.5217

[11] T.T. Pham, K.H. Nguyen, "Co ngót trong kết cấu bê tông", Nhà xuất bản Xây dựng, Hà Nội, 2026.

[12] Bộ Xây Dựng, *Chỉ dẫn kĩ thuật lựa chọn thành phần bê tông các loại*. Nhà xuất bản Xây dựng, 2000.

[13] Bộ Khoa Học Và Công Nghệ, "Hardened concrete – test method for compressive strength," Bộ Khoa học và Công nghệ, Hà Nội, Vietnamese National Standard TCVN 3118:2022, 2022.

[14] Bộ Khoa Học Và Công Nghệ, "Concrete – control and assessment of strength using moulded specimens," Bộ Khoa học và Công nghệ, Hà Nội, Vietnamese National Standard TCVN 10303:2025, 2025.

[15] Dassault Systèmes, *Abaqus 2024 documentation: embedded elements, rigid body definition, and element library*. Johnston, Rhode Island: Dassault Systèmes Simulia Corp., 2024. Accessed: Jul. 28, 2026.

[16] Dassault Systèmes, *Abaqus 2024 documentation: inelastic behavior and concrete damaged plasticity*. Johnston, Rhode Island: Dassault Systèmes Simulia Corp., 2024. Accessed: Jul. 28, 2026.

[17] J. Lubliner, J. Oliver, S. Oller, and E. Oñate, "A plastic-damage model for concrete," *Int. J. Solids Struct.*, vol. 25, no. 3, pp. 299–326, 1989
DOI: 10.1016/0020-7683(89)90050-4.

[18] J. Lee and G. L. Fenves, "Plastic-damage model for cyclic loading of concrete structures," *J. Eng. Mech.*, vol. 124, no. 8, pp. 892–900, Aug. 1998
DOI: 10.1061/(ASCE)0733-9399(1998)124:8(892).

[19] B. Alfarah, F. López-Almansa, and S. Oller, "New methodology for calculating damage variables evolution in plastic damage model for RC structures," *Eng. Struct.*, vol. 132, pp. 70–86, Feb. 2017
DOI: 10.1016/j.engstruct.2016.11.022

[20] British Standards Institution, "Eurocode 2: design of concrete structures – part 1-1: general rules and rules for buildings," British Standards Institution, London, British Standard BS EN 1992-1-1:2004, Dec. 2004
DOI: 10.3403/03178016u